Parametric Study on the Heat Management of Metal Hydride Tanks for Sustainable Building Applications

Gkanas, E., Khzouz, M., Skodras, G. & Makridis, S.

Gkanas, E, Khzouz, M, Skodras, G & Makridis, S 2018, Parametric Study on the Heat Management of Metal Hydride Tanks for Sustainable Building Applications. in International Journal of Computational Physics Series. 1 edn, vol. 1, Natural Science Simulations and Engineering Laboratory Limited, UK, pp. 13-29, International Conference on Computational Materials Science and Thermodynamic Systems, Cambridge, United Kingdom, 22/03/18.
https://dx.doi.org/10.29167/A1I1P13-29

DOI 10.29167/A1I1P13-29
IBSN 978-1-912532-00-1

Publisher: NSSEL Publishing

Parametric Study on the Heat Management of Metal Hydride Tanks for Sustainable Building Applications

Evangelos I. Gkanas[1*], Martin Khzouz[1], George Skodras[2] and Sofoklis Makridis[3]

[1]*Hydrogen for Mobility Lab, Institute for Future Transport and Cities, School of Mechanical, Automotive and Aerospace Engineering, Coventry University, Cheetah Road, Chamber House IV09, CV1 2TL, Coventry, UK.*

[2] *Novel & Clean Technologies Lab., Dept. of Mechanical Engineering, University of Western Macedonia, Mpakola & Sialvera, 501 00, Kozani, Greece.*

[3] *Department of Environmental and Natural Resources Management, University of Patras, 2 Seferi St., Agrinio, Greece*

*Email: evangelos.gkanas@coventry.ac.uk

Abstract: In the current work, a parametric numerical analysis of $MmNi_{4.6}Al_{0.4}$ is studied during the hydrogenation process; under effective heat management. A fully validated with solid experimental results mathematical model including the heat, mass and momentum conservation equations is introduced, described and incorporated on a Multiphysics software (COMSOL Multiphysics). The target of the current study was the storage of 200g of hydrogen per hydrogenation/dehydrogenation cycle within 5000s. The heat management during the hydrogenation process was performed by the usage of plain-embedded cooling tubes in combination with extended surfaces. The parameters examined in the current work were; the fin thickness, the fin number (metal hydride thickness) and the coolants' flowrate within the tubes. A non-dimensional parameter was utilised for the evaluation of the heat management process. The results showed that the optimum fin number was 60, in combination with fin thickness 5-8mm and the value of the heat transfer coefficient 2000-5000 $Wm^{-2}K^{-1}$.

Keywords: Hydrogen Storage; Heat Management; Heat and Mass Transfer; Metal Hydrides.

1 Introduction

The negative environmental impact of buildings, is directly connected to the energy consumption and the greenhouse gas emissions [1, 2]. The energy consumption in buildings in several advanced and developed countries has already exceeded the energy consumption of the industrial and transportation sector [3, 4]. The same trend is followed by several other under-development countries [5]. Hydrogen technologies can play a crucial role on the sustainability of the new generation of buildings, as they utilized for applications such as; grid stabilization, reserves for grid frequency and voltage regulation [6]. The storage of hydrogen to feed a fuel cell system is one of the drawbacks for the commercial implementation of hydrogen economy [7]. The storage of hydrogen in the interstitial sites of metals and the formation of metal hydrides is an efficient technique that allows the hydrogen storage under moderate temperature and pressure conditions [8-10]. There are certain parameters governing the thermodynamic performance of metal hydrides. The material-related parameters, such as; the thermal conductivity λ $(Wm^{-1}K^{-1})$, the heat capacity of the hydride C $(J\,mol^{-1}K^{-1})$, the enthalpy of hydride formation/deformation ΔH $(J\,mol^{-1})$, the entropy of hydride formation/deformation ΔS $(J\,mol^{-1}K^{-1})$, the hysteresis and slope [11, 12]. Furthermore, there are additional parameters related to the operation/design of the metal hydride beds, such as; the porosity of the metal hydride bed, the packing density, the temperature of operation, the geometry of the metal hydride vessel, the supply pressure and the heat management techniques [13, 14].

The limiting factor affecting and control the hydrogenation/dehydrogenation process is the rate of heat that is transferred to/from the metal hydride bed. During the hydrogenation process, the hydrogen atoms are diffusing within the metallic lattice and creating bonds with the metal atoms; thus, it is an exothermic process, with large amounts of heat produced during the formation of the hydride [15]. Those amounts of heat are forcing the equilibrium pressure to increase and consequently to reduce the driving force for the storage, which is the pressure difference [16]. Thus, the heat management of metal hydride tanks is a crucial process to maintain the rate of reaction and the solid-state hydrogen storage. In general, there are two main techniques for effective heat management of metal hydrides; internal and external heat management [17-19]. By considering the Fourier's law of conduction and accommodate to metal hydride beds, there are three ways to improve the heat transfer in a metal hydride bed; improvement of the overall thermal conductivity [20, 21], introduction of a large temperature difference inside the bed [22] and the reduction of the metal hydride thickness [23, 24].

In the current work, a numerical model describing the hydrogenation process of an AB_5 intermetallic ($MmNi_{4.6}Al_{0.4}$) is introduced and studied. The proposed mathematical model includes the heat, mass and momentum conservation equations. The numerical model was validated with solid experimental results extracted from a Sievert type apparatus. The metal hydride beds used in the current study are cylindrical, and the properties of commercial available SS 316L were also considered. The heat management consists of plain-embedded cooling tubes in combination with extended surfaces. Several parameters were considered, such as the fin thickness, the distance between the fins (fin number) and the coolants' flow rate within the cooling tubes. To evaluate the effect of the heat management process, a variable named as Non-Dimensional Conductance (NDC) is analysed and studied.

2 Methodology

In the current study, a commercial multiphysics software (COMSOL Multiphysics 5.3) utilized by solving simultaneously the heat, mass and momentum conservation equations. Before conducting these simulation runs the performance of the proposed numerical model was validated with solid experimental results for both the hydrogen storage capacity and the temperature distribution within the hydride. The expansion of packed beds during the hydrogenation process can produce additional stress on the vessel walls; therefore, for the numerical analysis, the reactors are assumed to be filled up to 50% at the beginning of the hydrogenation process. After the validation process, the simulation runs were conducted for all the suggested parameters of fin thickness, fin number and coolants' flow.

2.1 Model Assumptions

Several assumptions were considered to simplify the simulation process and listed as follows:

a) The temperature and pressure profiles are initially uniform.
b) The thermal conductivity and specific heat capacity of the hydride are constant during the hydrogenation process.
c) The medium is in local thermal equilibrium; which implies that there is no heat transfer between solid and gas phases
d) Hydrogen is treated as an ideal gas from a thermodynamic point of view.
e) The bed void fraction remains constant and uniform throughout the reaction.
f) The characteristics (the kinetics and thermal properties) of the bed are unaffected by the number of loading and unloading cycles.
g) The metal hydride bed fills the entire space between the cooling tubes (perfect packing condition).

2.2 Heat equation

Assuming thermal equilibrium between the hydride powder and hydrogen gas, a single heat equation is solved instead of separate equations for solid and gas phases:

$$(\rho \cdot Cp)_{eff} \cdot \frac{\partial T}{\partial t} + (\rho_g \cdot C_{p_g} \cdot \bar{v}_g) \cdot \nabla T + \nabla \cdot (\mathrm{k}_{\mathrm{eff}} \cdot \nabla T) = \mathrm{Q}_H \tag{1}$$

The term Q_H *(W/ m^3)* in Eq. 1 represents the heat that is generated during the hydrogenation process. The amount of heat that is been produced during the hydrogenation process depends on several thermophysical properties of the materials, such as the enthalpy of formation *ΔH (J/mol)*, the porosity of the material *ε,* the density change during the reaction (kg/m^3), the reaction rate (1/s) and the molecular mass of the stored gas (kg/mol).

The effective heat capacity is given by;

$$(\rho \cdot Cp)_{\mathrm{e}} = \varepsilon \cdot \rho_g \cdot C_{pg} + (1-\varepsilon) \cdot \rho_s \cdot C_{ps} \tag{2}$$

and the effective thermal conductivity is given by;

$$k_e = \varepsilon \cdot k_g + (1-\varepsilon) \cdot k_s \tag{3}$$

The terms ρ_g, C_{pg}, C_{ps} and *m* refer to the density of the gas phase (kg/m^3), the specific heat capacity of the gas phase (J kg^{-1}K^{-1}), the heat capacity of the solid phase and the kinetic term for the reaction respectively. The parameter that represents the void fraction is symbolized with *ε*. M_{H2} represents the molecular mass of hydrogen (kg mol^{-1}) and *T* represents the temperature (K).

2.3 Hydrogen Mass Balance

The equation that describes the diffusion of hydrogen mass inside the metal matrix is given by:

$$\varepsilon \cdot \frac{\partial(\rho_g)}{\partial t} + div(\rho_g \cdot \vec{v}_g) = \mp Q \tag{4}$$

Where, (-) refers to the hydrogenation process and (+) to the dehydrogenation process, v_g *(m/s^2)* is the velocity of gas during diffusion within the metal lattice (descripted in section 2.4) and *Q* is the mass source term describing the amount of hydrogen mass diffused per unit time and unit volume in the metal lattice.

2.4 Momentum equation

The velocity of a gas passing through a porous medium can be expressed by Darcy's law. By neglecting the gravitational effect, the equation that describes the velocity of gas inside the metal matrix is given by:

$$\vec{v}_g = -\frac{K}{\mu_g} \cdot grad(\vec{P}_g) \tag{5}$$

Where *K (m^2)* is the permeability of the solid and μ_g *(Pa s)* is the dynamic viscosity of gas and P_g *(Pa)* is the pressure of gas within the metal matrix.

2.5 Kinetic expression

The kinetic description for the hydrogenation process per unit time and volume is described by the following equation:

$$m_a = C_a \cdot \exp[-\frac{E_a}{R_g \cdot T}] \cdot \ln[\frac{p_g}{P_{eq}}] \cdot (\rho_{ss} - \rho_s) \tag{6}$$

Where ρ_s and ρ_{ss} are the density of the hydride at any time and at saturation state respectively. C_a (s^{-1}) refer to the pre-exponential constants for the hydrogenation process and the E_a $(J\ mol^{-1})$ is the activation energy for the hydrogenation.

2.6 Equilibrium Pressure.

To incorporate and consider the effect of hysteresis and the plateau slope for the calculation of the plateau pressure P_{eq}, the following equation was used:

$$\ln \frac{P_{eq}}{10^5} = \left\{ \left[\frac{\Delta \mathrm{H}}{RT} - \frac{\Delta S}{R} \right] + \left(\varphi_s \pm \varphi_0 \right) \cdot \tan \left[\pi \cdot \left(\frac{x}{x_{sat}} - \frac{1}{2} \right) \right] \pm \frac{S}{2} \right\} \tag{7}$$

The plateau slope is given by the flatness factors φ_s and φ_0 and S represents the hysteresis effect which is given by (lnP_{abs}/P_{des}) designated '+' for hydrogenation and '-' dehydrogenation, while x and x_{sat} are the local hydride concentration at any given time and at saturation respectively. For the studied material, the flatness factors and the hysteresis effects were measured experimentally by using the data collected from the hydrogenation kinetics and isotherms.

3 Validation of the numerical model

Validation of numerical results

To investigate the validity of the proposed model, experiments on a 0.8g sample of $MmNi_{4.6}Al_{0.4}$ powder were performed. The phase purity was validated by means of XRD (Rietveld Analysis). The pressure-composition-isotherm (PCI) hydrogenation measurements were performed on a commercial Sievert type apparatus provided by HIDEN Isochema (IMI Instruments). Both the hydrogenation and temperature behaviour of the material were recorded during the charging process at an initial hydrogen supply pressure of 12 bar. Fig. 1 shows the comparison of the temperature and hydrogenation profile during the hydrogenation process. The results of the numerical work compared to the experimental data present good agreement with a maximum deviation of less than 5%.

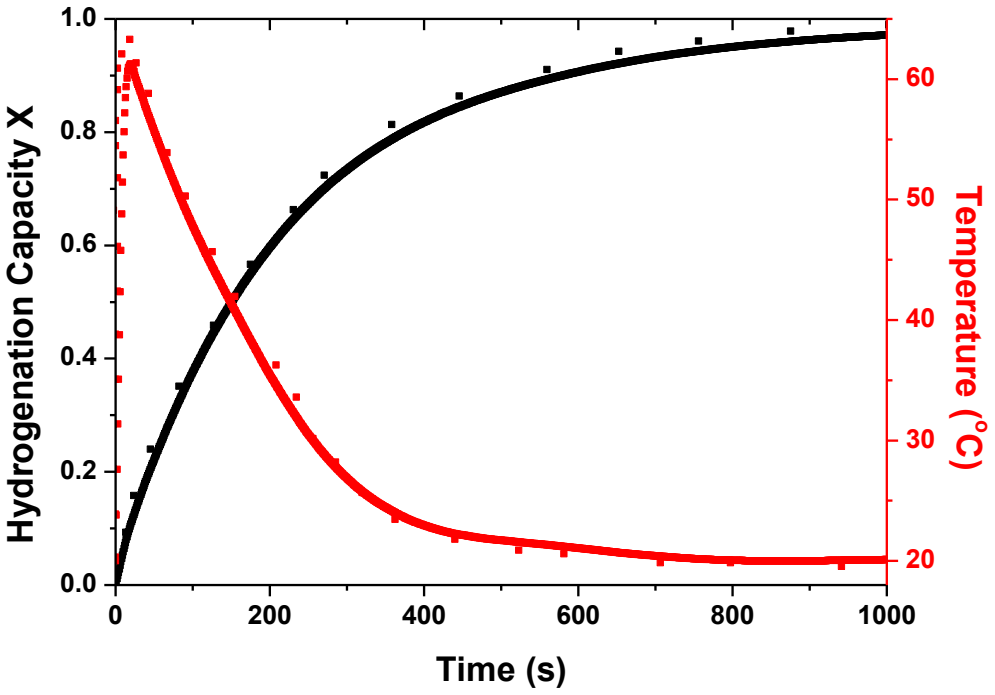

Fig.1 Validation of the predicted temperature profile (red) and the hydrogen storage capacity (black) for $MmNi_{4.6}Al_{0.4}$.

4 Tank Design Geometries

The metal hydride tanks are cylindrical. The properties of commercially available stainless steel (SS 316L) with wall thickness of 3mm were introduced for the tank definition. The amount of powder selected for the study was 12285.71 g, necessary to store up to 200g of hydrogen per cycle. The cylinders chosen for the study had 0.8m length and 0.052m radius. For the heat management process, a combination of cooling tubes with extended surfaces studied. Five cooling tubes placed along the cylindrical tank; one tube placed in the middle and the other four placed on a co-central distribution. Fig. 2 shows the geometry of the cooling tubes and the fins considered. The fins were selected to have five openings (holes) to allow the cooling tubes to penetrate; furthermore, four openings were also considered mainly for two reasons; to allow the powder to move through the 'chambers' that were formatted between two adjacent fins for the packing reasons, and to avoid any issues due to the expansion of the hydride during the hydrogenation process.

4.1 Optimisation Factors and Control Parameters

The charging/discharging time is of major importance for the effective performance of a metal hydride tank. The purpose of the present optimization process is to obtain the system's parameters that lead to the minimum charging/discharging time (t_s). In the current analysis, the charging/discharging time (t_s) is defined as the time required for the average reacted fraction to increase from 0.1 to 0.9 during the hydrogenation process. The parameters examined are: a) the fin thickness, b) the number of fins and c) the coolants flow within the tubes which is represented by the heat transfer coefficient h_t (W/m^{2}K).

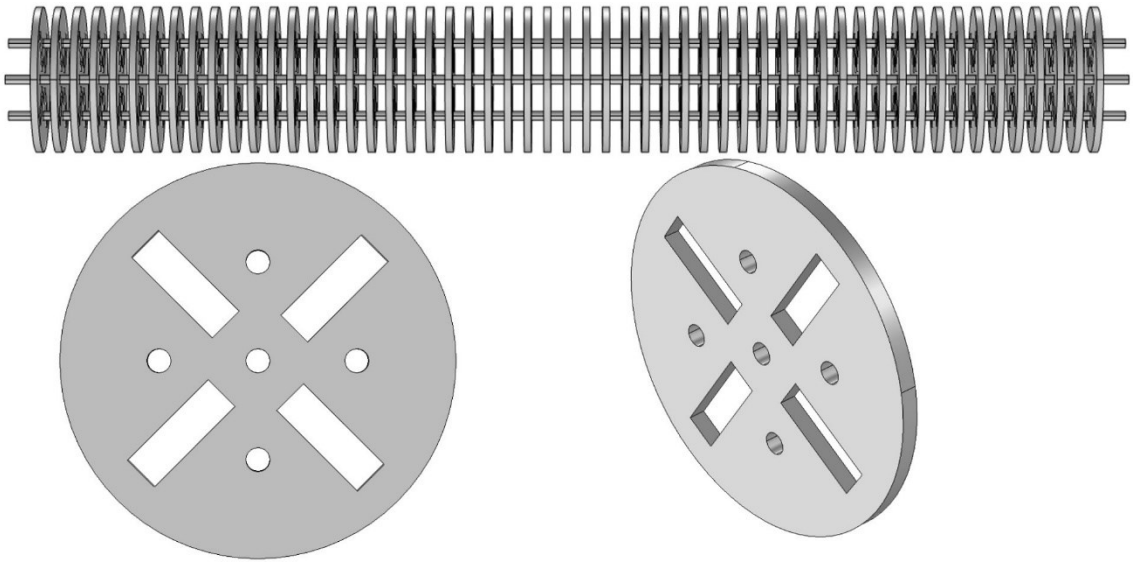

Fig.2 Geometry of the cooling tubes and the extended surfaces.

Table 1 presents all the control factors and the values used for the current study.

Table 1. Control factors and cases considered for the study

Fin Thickness (mm)	Number of Fins	Heat Transfer Coefficient ($Wm^{-2}K^{-1}$)
2	50-55-60-65-70	500-1000-2000-5000
3	50-55-60-65-70	500-1000-2000-5000
5	50-55-60-65-70	500-1000-2000-5000
8	50-55-60-65-70	500-1000-2000-5000

4.2 Non- Dimensional Conductance (NDC)

The reaction rate for the hydrogenation/dehydrogenation depends on the heat transfer parameters. In the current work, heat exchangers coupled with extended surfaces are used to enhance the hydrogenation of $MmNi_{4.6}Al_{0.4}$. When using a heat exchanger, there are several parameters that influence the rate of heat transfer such as; the coolant temperature, coolant flow rate, contact resistance, metal hydride thickness and the thermal conductivity of the metal hydride bed. To monitor the influences of the above parameters on the heat transfer performance a Non-Dimensional Conductance (NDC) parameter can be considered [23]. The NDC is defined as the ratio of the maximum heating rate that can be removed from the metal hydride to the heat rate that would be generated for a specified thickness of the hydride to store hydrogen up to 90% of its maximum theoretical performance during a desirable time and its given by the following expression.

$$NDC = \frac{\left(\frac{T_{MH,\max} - T_{cool}}{\frac{1}{h_t} + R_{tc} + \frac{L}{\lambda}} \right)}{\left(\frac{\Delta H \cdot (\text{wt}\%) \cdot \rho}{MW_{H2}} \cdot \frac{L}{t_{des}} \right)} \quad (8)$$

Higher values of NDC result in larger heat transfer rates. $T_{MH,max}$ *(K)* is the temperature of the metal hydride at the end of the pressure increase process and it is an indirect measurement of the pressure. T_{cool} *(K)* is the temperature of the coolant that flows within the heat management tubes and a higher NDC number can be achieved by reducing the coolant temperature. The heat transfer coefficient is represented by h_t *(W/m^{2}K)* and is directly related to the effect of the coolant flow rate. R_{tc} *(mm^{2}K/W)* is the contact resistance between the metal hydride powder and the wall of the heat management tubes and it depends on the hydride powder properties (grain size and packing density). *L (mm)* is the hydride layer thickness. In the current work, the metal hydride thickness is defined as the distance between the centers of two adjacent coolant tubes and consists of the metal hydride, the contact resistance and the wall of the coolant tube. The denominator in Eq. 8 is the average heat generation rate if the metal hydride of thickness *L* is hydride within a desired filling time t_{des}. In the current analysis, the desired time t_{des} was selected 5000s.

5 Results and Discussion

5.1 Hydrogenation behaviour of $MmNi_{4.6}Al_{0.4}$

The initial temperature of the material for all the studied cases was 20ºC, same as the initial temperature of the coolant. Hydrogen supply pressure was 15 bar; the pressure that a commercial electrolyser can supply. Four different fin thicknesses were examined; *2-3-5 and 8 mm.* For each one of the thicknesses, five different values of fin number were selected (*50-55-60-65 and 70 fins*) corresponding to different values of metal hydride thickness. In the current study, the metal hydride thickness is defined as the distance between the centres of two adjacent fins. In addition, the effect of the coolants' flowrate was examined, by considering four different values of the heat transfer coefficient: 500-1000-2000 and 5000 W m^{-2}K^{-1}. Out of the mathematical point of view, the heat transfer coefficient is the ratio between the heat flux to the temperature change. This temperature change ΔT is the driving force for the transfer of the thermal energy. Fig. 3 presents the hydrogenation response of $MmNi_{4.6}Al_{0.4}$ in respect to the different values of the heat transfer coefficient chosen for the current study (*500-1000-2000 and 5000 W m^{-2}K^{-1}*) for the case of fin thickness 5mm. The maximum time considered for the hydrogenation process to reach X=0.9 (hydrogenation fraction) was 5000s. For the lower values of the heat transfer coefficient (*500 and 100 W m^{-2}K^{-1}*) the hydrogenation does not reach the target (X=0.9) within 5000s for all the cases of fin number. When the heat transfer coefficient increases to 2000 W m^{-2}K^{-1}, the hydrogenation for all the cases of fin number reaches the desired fraction X=0.9 within the time frame of 5000s. Furthermore, as the fin number increases, the hydrogenation becomes faster. When the fin number increases from 50 to 55, the decrease on the hydrogenation time is low (15 s); but when the fin number increase to 60, the hydrogenation becomes faster comparing to the case of 55 fins (120 s). A further increase of the fin number to 65 and 70, does not significantly improve the hydrogenation time. In addition, for the case of the heat transfer coefficient 5000 W m^{-2}K^{-1}, it appears that the increase over 65 fins might cause a 'negative' effect on the hydrogenation time. From the above, it can be extracted that the increase of the heat transfer coefficient can enhance the hydrogenation process; the same with the increase of the fin number up to 60. A further increase of the fin number does not improve the hydrogenation rate. This behaviour can be explained from the thermodynamic nature of the hydrogenation process. During the hydrogen

storage and the creation of the metal-hydrogen bonds (hydride formation), substantial amounts of thermal energy are produced. As the coolant flowrate increases (larger heat transfer coefficient), the system is capable to remove faster the produced thermal energy. Furthermore, the increase of the fin number results on the decrease of the metal hydride thickness. Up to a certain value of metal hydride thickness, the reduction leads to the increase of the hydrogenation rate. On the other hand, increase of fins over 60, does not improve the reaction; a limitation mechanism begins, where the coolants flow rate seems to dominate in that region [19].

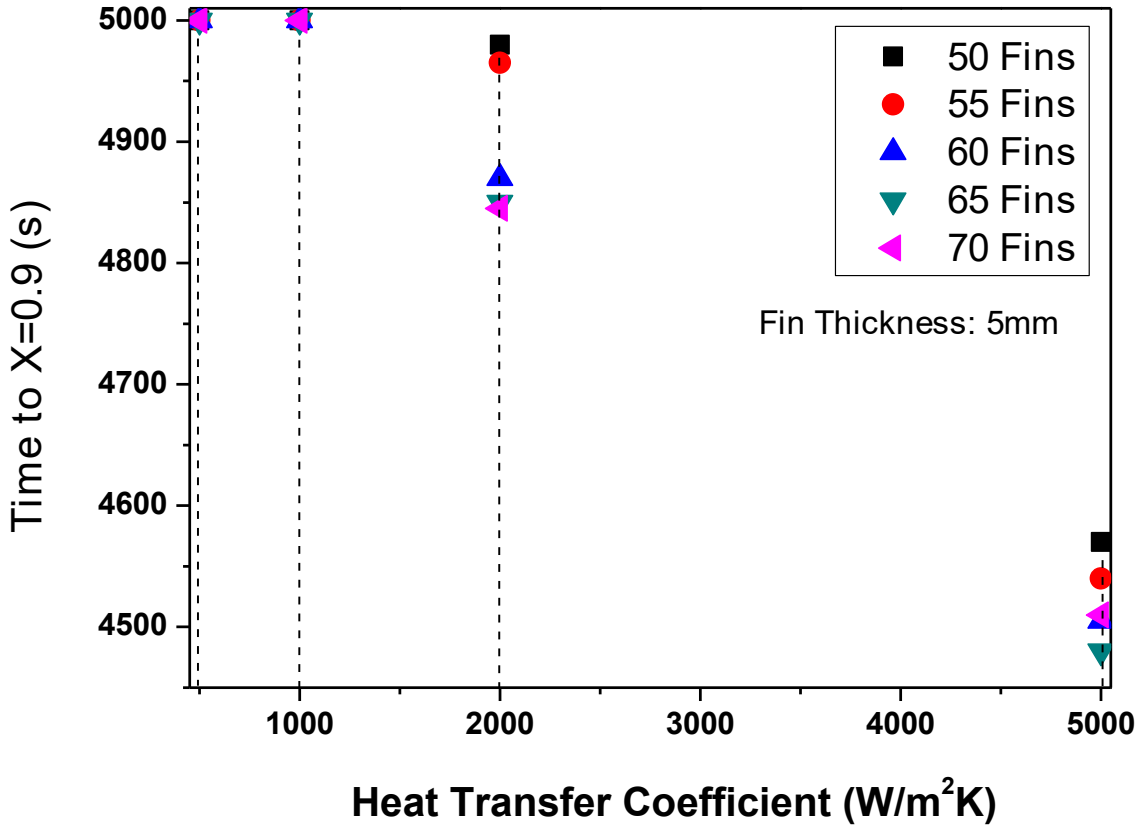

Fig.3. Hydrogenation response of $MmNi_{4.6}Al_{0.4}$ when using fins with thickness 5mm for the heat management process, for all the different fin number and all the values of the heat transfer coefficient.

5.2 Effect of the metal hydride thickness on the hydrogenation behaviour of $MmNi_{4.6}Al_{0.4}$

According to the analysis described above, when the heat transfer coefficient reaches 2000 and 5000 W $m^{-2}K^{-1}$, the reaction for the hydrogen storage becomes faster and the material is able reach the hydrogenation fraction X=0.9 in less than 5000s. By considering only those two values, a comparison study is performed in terms of the effect that the fin thickness adds to the hydrogenation behaviour. Fig. 4a shows the hydrogenation behaviour (time to reach X=0.9) for all the number of fins and fin thicknesses when the heat transfer coefficient is 2000 W $m^{-2}K^{-1}$, while Fig. 4b shows the hydrogenation behaviour when the heat transfer coefficient is 5000 W $m^{-2}K^{-1}$.

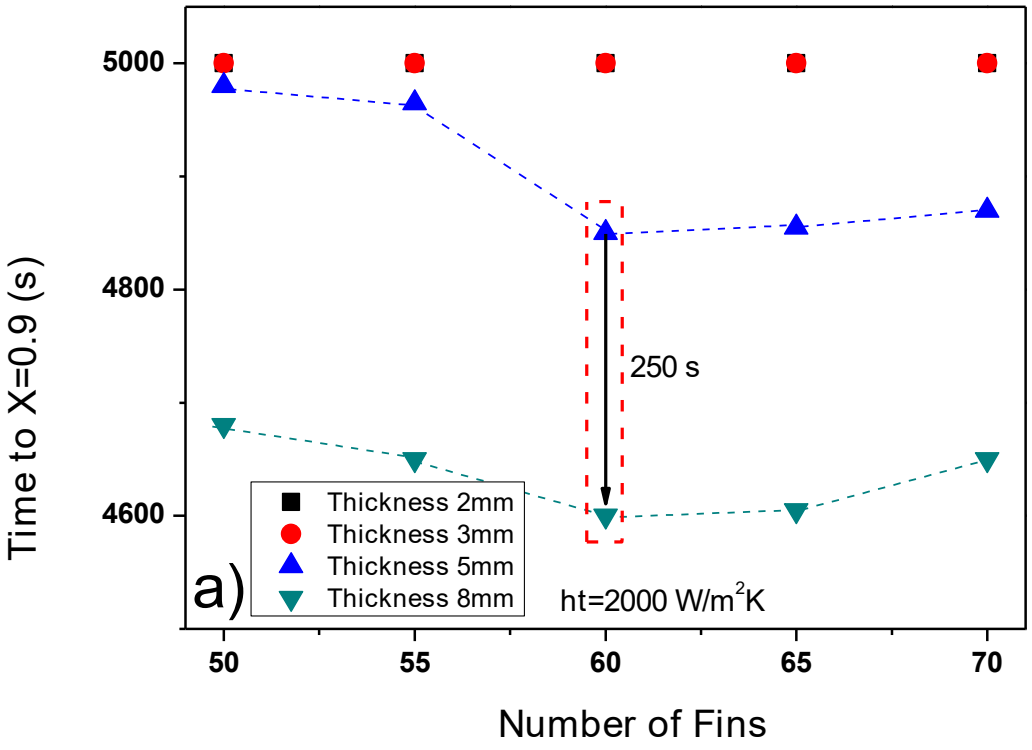
Time to X=0.9 (s)
5000
4800
4600
50
55
60
65
70
Number of Fins
250 s
Thickness 2mm
Thickness 3mm
Thickness 5mm
Thickness 8mm
a)
ht=2000 W/m²K

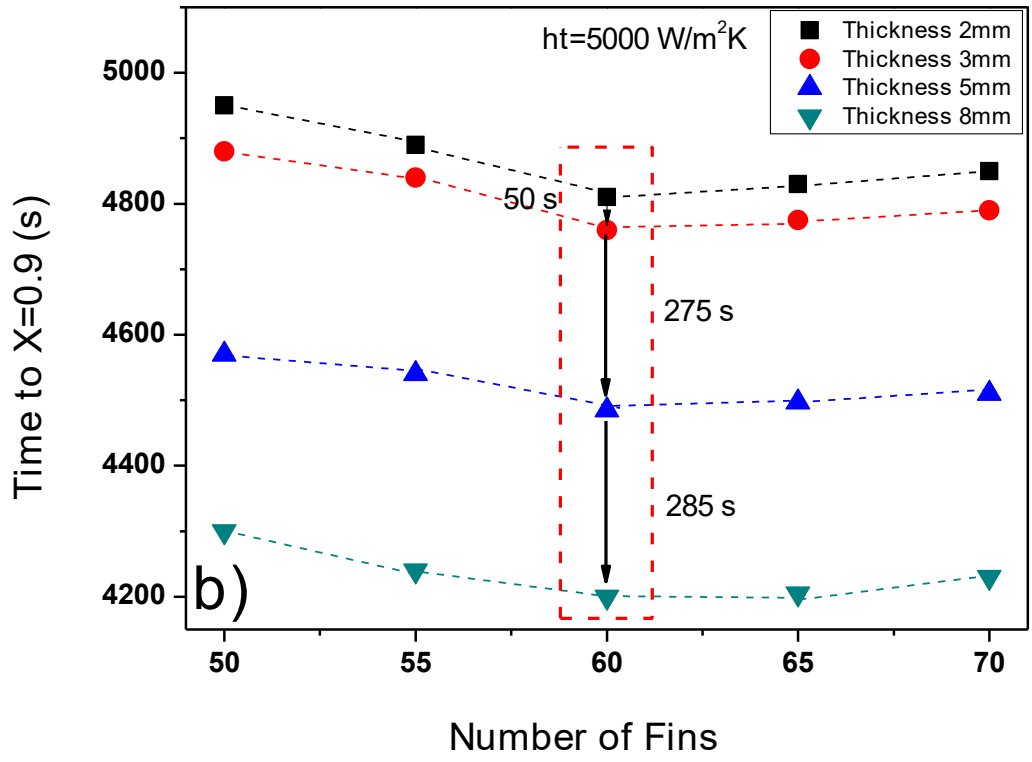
Time to X=0.9 (s)
5000
4800
4600
4400
4200
50
55
60
65
70
Number of Fins
ht=5000 W/m²K
Thickness 2mm
Thickness 3mm
Thickness 5mm
Thickness 8mm
50 s
275 s
285 s
b)

Fig.4. Hydrogenation response of $MmNi_{4.6}Al_{0.4}$ during the heat management process, for all the different fin number and thicknesses, when the heat transfer coefficient is 2000 W $m^{-2}K^{-1}$ (4a) and 5000 W $m^{-2}K^{-1}$ (4b).

When the heat transfer coefficient is 2000 W $m^{-2}K^{-1}$, for the fin thickness of 2 and 3mm, the material is not able to reach X=0.9 within 5000s. As the fin thickness increases to 5 and 8mm, the material stores that amount of hydrogen in the desired time. For the fin thickness of 5mm, as the number of fins increases, the reaction becomes faster until the value of 60 fins, where the minimum charging time is obtained (4850s). The increase of the fin number to 65 and 70 does not further improve the reaction rate. The same behaviour is observed for the case of the heat transfer coefficient 5000 W $m^{-2}K^{-1}$. The hydrogenation time reaches the minimum value when using 60 fins (4485s) and further increase to 65 and 70 fins does not accelerate the reaction.

When using 60 fins, for the case of heat transfer coefficient 2000 W $m^{-2}K^{-1}$ the increase of the fin thickness from 5 to 8mm will result on a drop of the hydrogenation time of more than 4min (250s). When the heat transfer coefficient is 5000 W $m^{-2}K^{-1}$ and the fin number is 60, the increase of the fin thickness from 2 to 3mm will result on a small drop of the hydrogenation time less than 1min (50s), whereas the increase of the fin thickness from 3 to 5mm will reduce the charging time over 4.5min. Finally, the increase of the thickness to 8mm will cause a reduction of the charging time of more than 4.5min (285s).

Fig.5 presents the variation of the hydrogenation time (time to X=0.9) with the Non-Dimensional Conductance (NDC) for the case of fin thickness 5–8mm and the value of heat transfer coefficient 2000-5000 W $m^{-2}K^{-1}$ respectively. For all the cases, when the fin number increases to 60 the hydrogenation time drops and the NDC also increases. The NDC is the maximum heating rate that can be removed from the metal hydride to the heating rate generated from a specified metal hydride thickness for the hydride to store 90% of its maximum theoretical performance. When the fin number increases to 65-70 the hydrogenation time does not drop and furthermore, the NDC values are almost the same. This behaviour indicates that when utilising 60 fins in the current system, the maximum amount of the generated heat can be removed from the system and due to the exothermic nature of the hydrogenation, the reaction will proceed faster. When the metal hydride thickness decreases (the fin number increases) below a threshold, the amount of heat that is removed from the system does not significantly change, indicating a limitation on the heat transfer mechanism.

Fig. 6 presents the comparison between the amount of hydrogen stored at the end of the desired time (5000s) and the NDC. Fig. 6a shows the comparison for the case of heat transfer coefficient 2000 W $m^{-2}K^{-1}$, while Fig.6b presents the comparison for the case of heat transfer coefficient 5000 W $m^{-2}K^{-1}$. The results showed that a charging time of 5000s is not achievable for the case of fin thickness 2 and 3mm, when the heat transfer coefficient is 2000 W $m^{-2}K^{-1}$. For thicknesses 5 and 8 mm, the material is able to reach the desirable charging time. For the case of 5000 W $m^{-2}K^{-1}$ the desired charging time is achieved for all the cases of fin thicknesses and fin number.

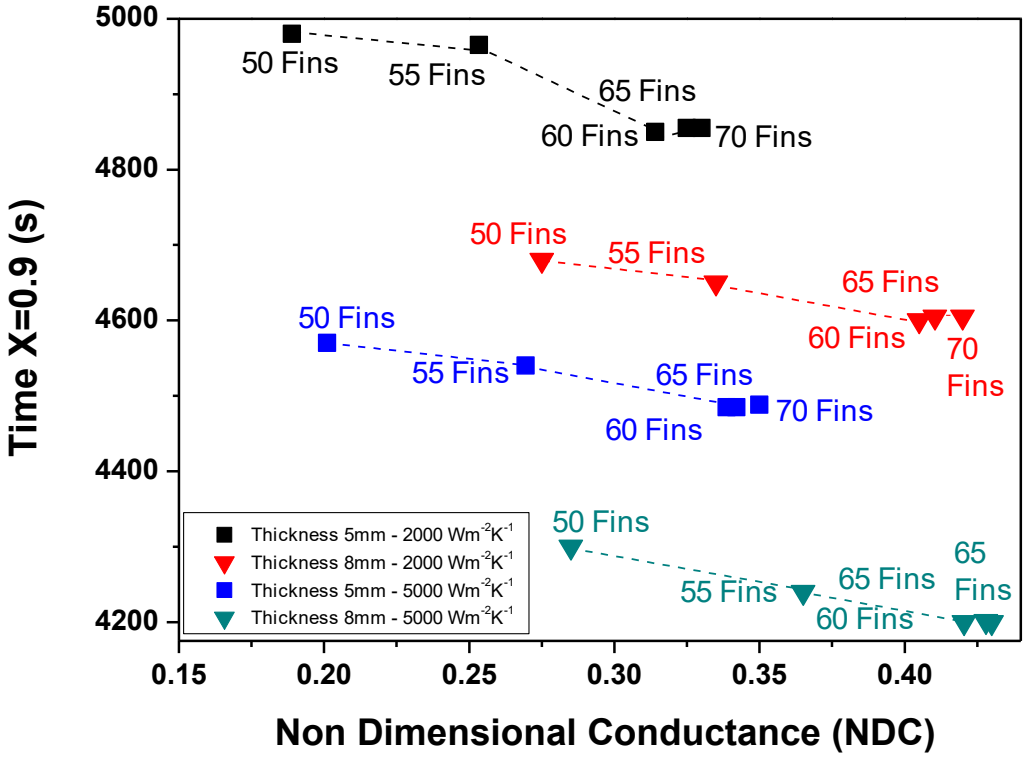

Fig. 5. Variation of the hydrogenation time (time to X=0.9) with the Non-Dimensional Conductance (NDC) for the case of fin thickness 5–8mm and the value of heat transfer coefficient 2000-5000 W $m^{-2}K^{-1}$ respectively

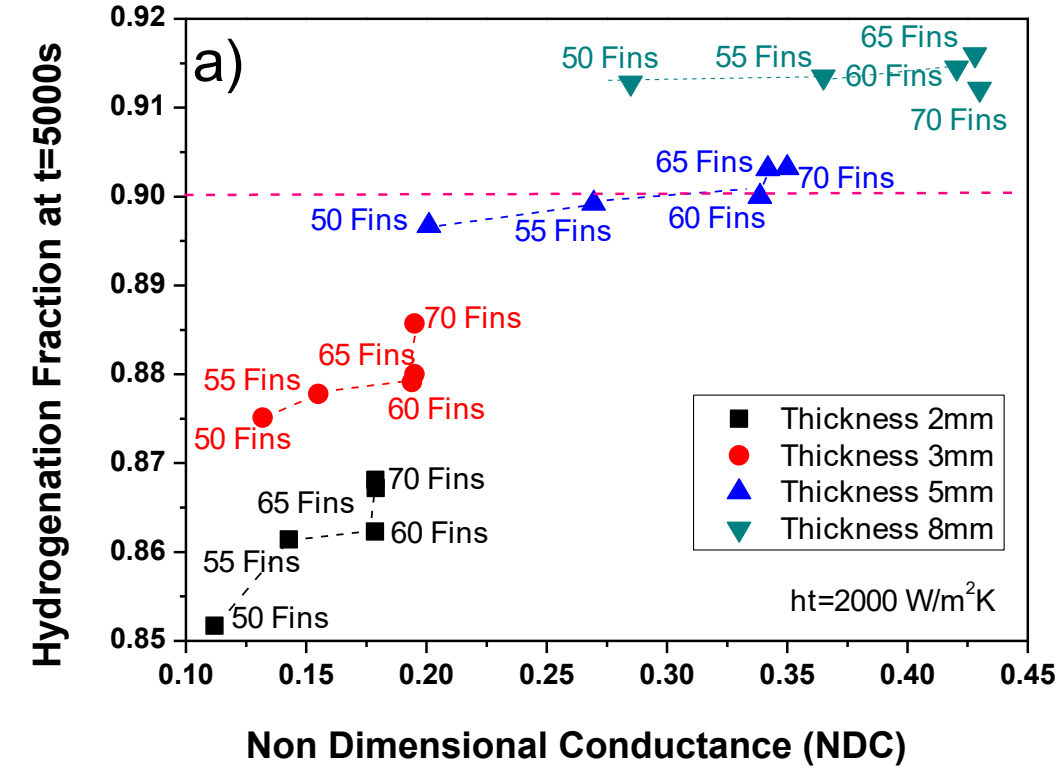
a)
Hydrogenation Fraction at t=5000s
Non Dimensional Conductance (NDC)
0.92
0.91
0.90
0.89
0.88
0.87
0.86
0.85
0.10
0.15
0.20
0.25
0.30
0.35
0.40
0.45
50 Fins
55 Fins
65 Fins
60 Fins
70 Fins
Thickness 2mm
Thickness 3mm
Thickness 5mm
Thickness 8mm
ht=2000 W/m2K

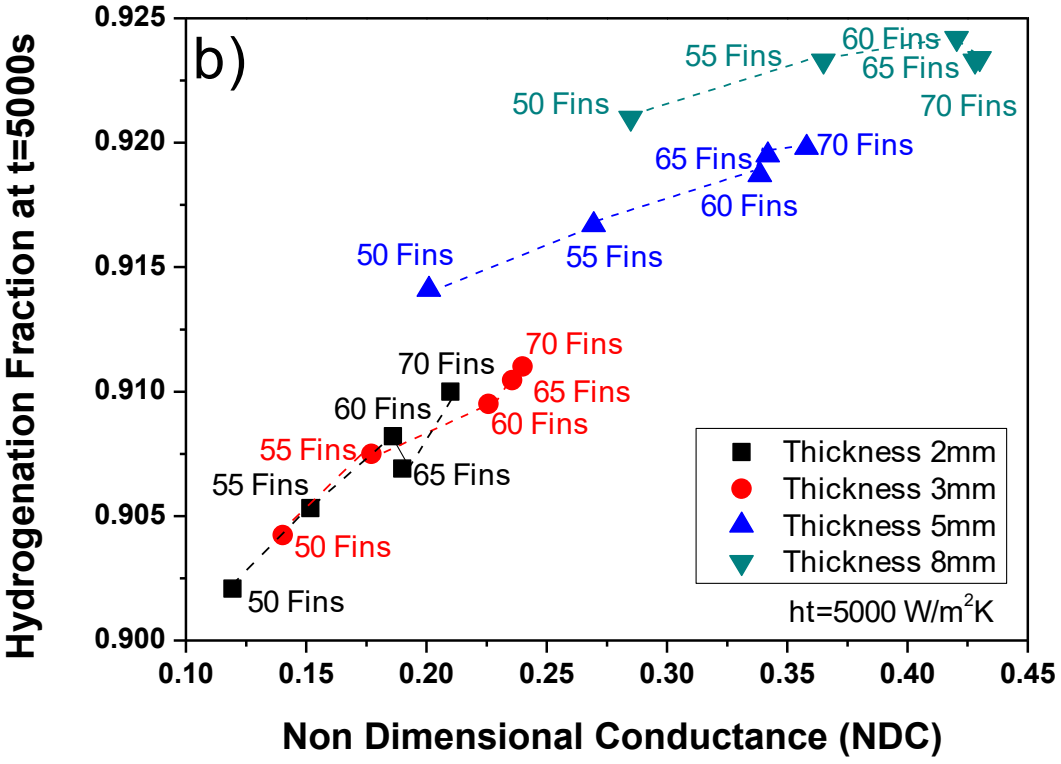
b)
Hydrogenation Fraction at t=5000s
Non Dimensional Conductance (NDC)
0.925
0.920
0.915
0.910
0.905
0.900
0.10
0.15
0.20
0.25
0.30
0.35
0.40
0.45
50 Fins
55 Fins
60 Fins
65 Fins
70 Fins
Thickness 2mm
Thickness 3mm
Thickness 5mm
Thickness 8mm
ht=5000 W/m2K

Fig.6 Comparison between the amount of hydrogen stored at the end of the desired time (5000s) and the NDC. Fig. 6a shows the comparison for the case of heat transfer coefficient 2000 W $m^{-2}K^{-1}$, while Fig.6b presents the comparison for the case of heat transfer coefficient 5000 W $m^{-2}K^{-1}$

5.3 **Hydrogenation Kinetics and Temperature Profile**

Fig. 7a presents the bed average temperature evolution of the hydride during the hydrogenation process, when the hydrogenation is performed under the optimum operational conditions described above. The number of fins was selected 60, whereas for the fin thickness two values were selected; 5 and 8mm. Finally, two values were also selected for the heat transfer coefficient (2000 and 5000 W $m^{-2}K^{-1}$). The temperature at the beginning of the hydrogenation process increases due to the highly exothermic process and reaches a maximum point. After that, due to the heat management process the temperature drops and tends to reach the temperature of the coolant.

The temperature for $MmNi_{4.6}Al_{0.4}$ rises rapidly and reaches a maximum between 57-63^{o}C for all the presented cases during the first 150s of the reaction, due to the low thermal conductivity of the hydride powders that restrict to the effective heat removal; at that time the hydride stores an amount of hydrogen at a hydrogenation fraction X=0.16 (16% of the theoretical maximum amount of hydrogen that can be stored) as presented in Fig. 7b. During the first stage of the hydrogenation process, the pressure difference is the major factor for the rapid storage. The temperature rise increases the equilibrium pressure and as a result, the driving potential for the hydrogenation process decreases; during the second stage of the hydrogenation the circulating coolant removes the produced heat from the tank and reduces the temperature. As a result, the driving potential starts to increase and further storage takes place and this process continues until the maximum capacity achieved. Thus; during the second stage of the hydrogenation process the heat transfer plays the key role.

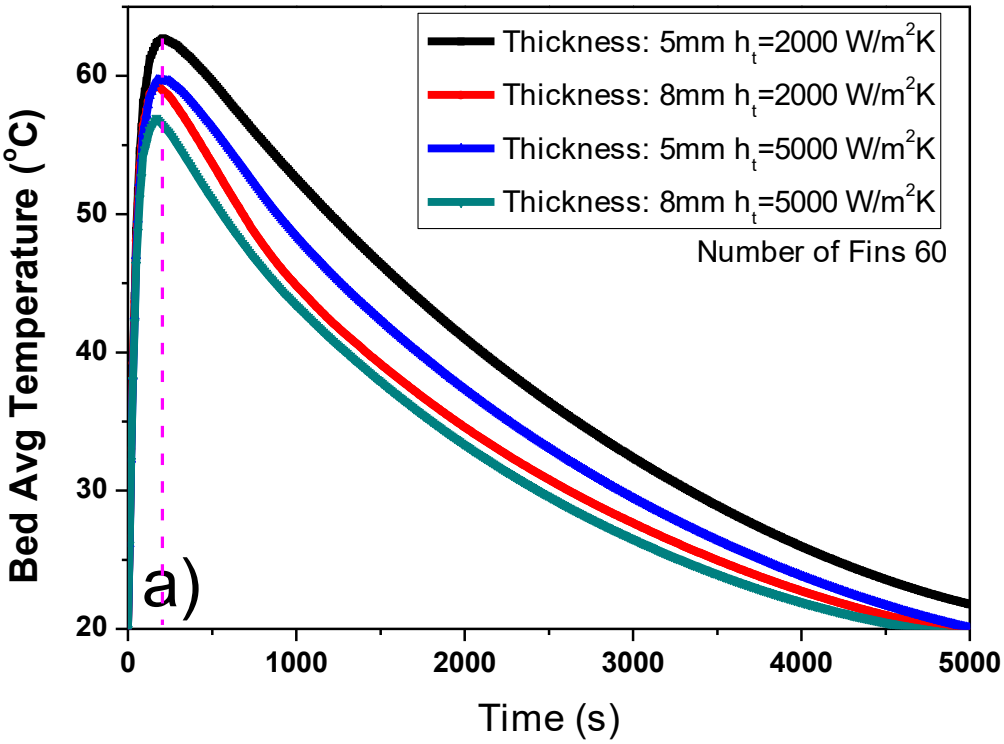
Bed Avg Temperature (°C)
Time (s)
Thickness: 5mm h_t=2000 W/m²K
Thickness: 8mm h_t=2000 W/m²K
Thickness: 5mm h_t=5000 W/m²K
Thickness: 8mm h_t=5000 W/m²K
Number of Fins 60
a)
20
30
40
50
60
0
1000
2000
3000
4000
5000

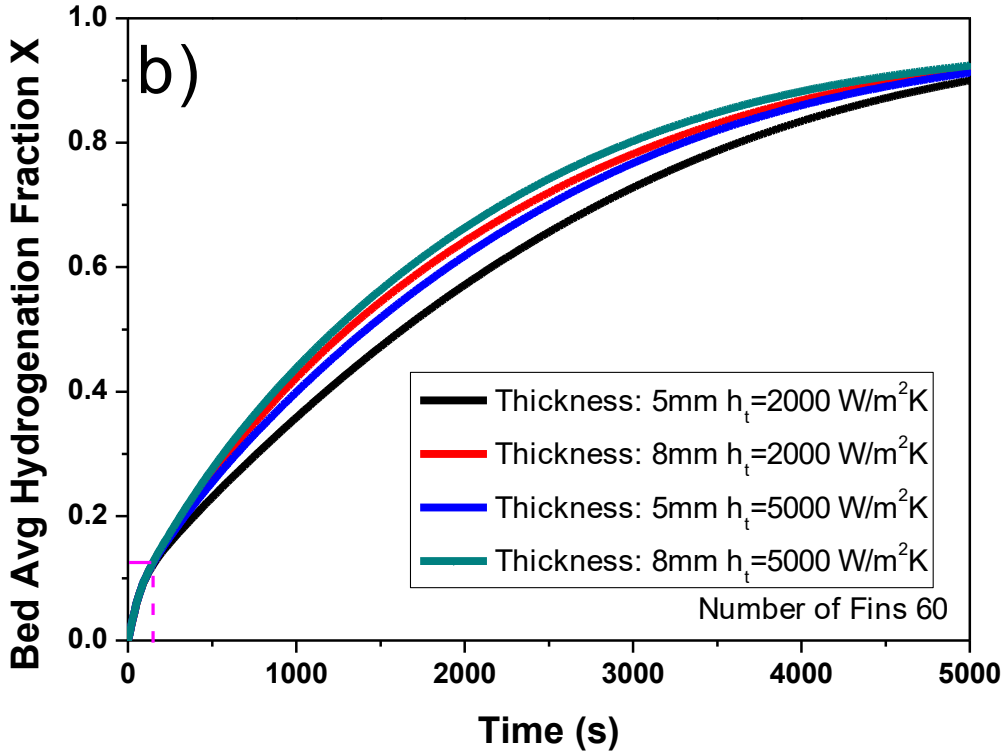
Bed Avg Hydrogenation Fraction X
Time (s)
b)
Thickness: 5mm h_t=2000 W/m²K
Thickness: 8mm h_t=2000 W/m²K
Thickness: 5mm h_t=5000 W/m²K
Thickness: 8mm h_t=5000 W/m²K
Number of Fins 60
0.0
0.2
0.4
0.6
0.8
1.0
0
1000
2000
3000
4000
5000

Fig. 7. Bed average temperature evolution (7a) and bed average hydrogenation fraction (7b) of the hydride during the hydrogenation process when the hydrogenation is performed under the optimum operational conditions.

6 Conclusions

The work presented in this study introduces and analyses the heat management of cylindrical metal hydride tanks, where $MmNi_{4.6}Al_{0.4}$ is utilised as the operating hydride. The target of the current work was the storage of 200g of hydrogen in less than 5000s. A mathematical model, including the heat, mass and momentum conservation equations was proposed. A validation process with experimental results was also performed. For the validation, the storage behaviour, the temperature distribution and the heat transfer were considered. The heat management of the metal hydride tank used plain-embedded cooling tubes coupled with extended surfaces (fins). Several parameters were examined; the fin thickness, the number of fins and the coolants flow rate (heat transfer coefficient).

Additionally, a Non-Dimensional Conductance parameter was introduced for the evaluation of the heat management. The results of the hydrogenation behaviour showed that the optimum number of fins was 60. Further increasing to 65 and 70 didn't improve the hydrogenation. The optimum fin thicknesses were selected 5 and 8mm. Below those values (2 – 3mm) the hydrogenation couldn't reach the 90% of the theoretical capacity in less than 5000s. Finally, the heat transfer coefficient to achieve the hydrogenation time can be 2000 – 5000 W $m^{-2}K^{-1}$.

Acknowledgments

The current work was financially partially supported from Coventry University ECR Funding Schemes

Nomenclature

C_a	*Absorption Reaction Constant, s^{-1}*
C_d	*Desorption Reaction Constant, s^{-1}*
C_p	*Specific Heat, J/kg-K*
E_a	*Activation Energy for Absorption, $J/molH_2$*
h	*Heat Transfer Coefficient, W/m^2K*
k	*Thermal Conductivity, W/m-K*
K	*Permeability, m^2*
M	*Molecular Weight, kg/mol*
m	*Kinetic Expression*
n	*Number of Hydrogen Moles*
P	*Pressure, bar*
R	*Gas Global Constant, J/mol-K*
t	*Time (s)*
T	*Temperature (K)*
v	*Gas Velocity, m/s*
V	*Volume, m^3*

Subscripts

a	*Absorption*
d	*Desorption*
e	*Effective*
eq	*Equilibrium*
f	*External Cooler*
g	*Gas*
i	*Initial*
s	*Solid*
ss	*Saturation*

Greek Letters

ε	*Porosity*
μ	*Dynamic Viscosity, kg/ms*
ρ	*Density, kg/m3*
ΔH	*Reaction Enthalpy, J/mol*
ΔS	*Reaction Entropy, J/mol-K*

References

[1] Gkanas, E.I., Khzouz, M., Panagakos, G., Statheros, T., Mihalakakou, G., Siasos, G.I., Skodras, G., Makridis, S.S., 2018. *Energy* **142**, 518–530.

[2] Gkanas, E.I., Steriotis, T.A., Stubos, A.K., Myler, P., Makridis, S.S., 2015. *Appl. Therm. Eng.* **74**, 36–46.

[3] Bland, A., Khzouz, M., Statheros, T., Gkanas, E.I., 2017. *Buildings* **7**.

[4] Markovska, N., Klemeš, J.J., Duić, N., Guzović, Z., Mathiesen, B.V., Lund, H., Yan, J., 2014. *Appl. Energy* **135**, 597–599.

[5] Deng, S., Wang, R.Z., Dai, Y.J., 2014. *Energy* **71**, 1–16.

[6] Verbecke, F., Vesy, B., 2013. *Int. J. Hydrogen Energy* **38**, 8053–8060.

[7] Makridis, S.S., Gkanas, E.I., Panagakos, G., Kikkinides, E.S., Stubos, A.K., Wagener, P., Barcikowski, S., 2013. *Int. J. Hydrogen Energy* **38**, 11530–11535.

[8] Gaboardi, M., Amadé, N.S., Aramini, M., Milanese, C., Magnani, G., Sanna, S., Riccò, M., Pontiroli, D., 2017. *Carbon* **120**, 77–82

[9] Delogu, F., Mulas, G., Garroni, S., 2009. Appl. Catal. A Gen. **366**, 201–205.

[10] Gkanas, E.I., Khzouz, M., 2017. Renew. Energy **111**, 484–493.

[11] Koultoukis, E.D., Gkanas, E.I., Makridis, S.S., Christodoulou, C.N., Fruchart, D., Stubos, A.K., 2014. *Int. J. Energy Res*. **38**, 477–486.

[12] Melnichuk, M., Silin, N., 2012. *Int. J. Hydrogen Energy* **37**, 18080–18094.

[13] Muthukumar, P., Satheesh, A., Linder, M., Mertz, R., Groll, M., 2009. *Int. J. Hydrogen Energy* **34**, 7253–7262.

[14] Muthukumar, P., Linder, M., Mertz, R., Laurien, E., 2009. *Int. J. Hydrogen Energy* **34**, 1873–1879.

[15] Gkanas, E.I., Makridis, S.S., Stubos, A.K., 2013. *Comput. Aided Chem. Eng*. **32**, 379–384.

[16] Muthukumar, P., Singh Patel, K., Sachan, P., Singhal, N., 2012. *Int. J. Hydrogen Energy* **37**, 3797-3806.

[17] Mazzucco, A., Dornheim, M., Sloth, M., Jensen, T.R., Jensen, J.O., Rokni, M., 2014. *Int. J. Hydrogen Energy* **39**, 17054-17074.

[18] Talagañis, B.A., Meyer, G.O., Oliva, D.G., Fuentes, M., Aguirre, P.A., 2014. *Int. J. Hydrogen Energy* **39**, 18997–19008.

[19] Gkanas, E.I., Grant, D.M., Stuart, A.D., Eastwick, C.N., Book, D., Nayebossadri, S., Pickering, L., Walker, G.S., 2015. *J. Alloys Compd*. **645**, S18–S22.

[20] Gkanas, E.I., Grant, D.M., Khzouz, M., Stuart, A.D., Manickam, K., Walker, G.S., 2016. *Int. J. Hydrogen Energy* **41,** 10795-10810.

[21] Sánchez, A.R., Klein, H.-P., Groll, M., 2003. *Int. J. Hydrogen Energy* **28**, 515–527.

[22] Gambini, M., Stilo, T., Vellini, M., Montanari, R., 2017. *Int. J. Hydrogen Energy* **42**, 16195-16202.

[23] Visaria, M., Mudawar, I., Pourpoint, T., Kumar, S., 2010. *Int. J. Heat Mass Transf*. **53**, 2229–2239.

[24] Jemni, A., Ben Nasrallah, S., 1995. *Int. J. Hydrogen Energy* **20**, 43–52.